PHYSICAL REVIEW A, VOLUME 62, 023809

Mazer action in a bimodal cavity

R. Arun,[1] G. S. Agarwal,[1,2] M. O. Scully,[2,3] and H. Walther[2,4]
[1]*Physical Research Laboratory, Navrangpura, Ahmedabad 380 009, India*
[2]*Max-Plank Institut Für Quantenoptik, 85748 Garching, Germany*
[3]*Department of Physics, Texas A&M University, College Station, Texas 77843*
[4]*Sektion Physik, Ludwig-Maximilians-Universität, München, Germany*
(Received 12 January 2000; published 19 July 2000)

The work of Meyer, Scully, and Walther [Phys. Rev. A **56**, 4142 (1997)] is generalized to study the operation of a two-mode mazer with particular reference to the question of mode-mode correlations. The explicit expression for the detailed balance steady-state photon distribution has been derived. It is shown that the two-mode mazer exhibits much stronger sub-Poissonian statistics for each mode. The photon-number distributions are found to be quite sensitive to the presence of blackbody photons in the cavity. The interferences among contributions from different dressed states enable one to obtain the phase of the transmission amplitude of finding the atom in the initial excited state by considering a set of two measurements involving two different initial states of the atom-field system.

PACS number(s): 42.50.Vk, 42.50.Dv, 03.75.−b

I. INTRODUCTION

Since the early realization [1] of micromaser, the interaction of atoms with fields in high quality cavities continues to attract a great deal of attention [2]. The operation of micromazer has been explained [3,4] and many features of the characteristics of the field in the cavity have been predicted. These include sub-Poissonian statistics [3,4], the trapping states [5], and unusual types of diffusion of the field [6]. All these characteristics depend in important manner on parameters such as atomic flux, quality factor, etc. Recently in a remarkable experiment [7] the trapping states have also been seen. The work on micromasers has been generalized in many different directions. For example, the two-photon micromaser as well as the microlaser were realized [8,9]. Further the theory was extended to three-level systems [10].

When the micromaser is pumped by ultracold (laser cooled) atoms [11], quantization of external motion of atoms becomes necessary. This quantization of center-of-mass (c.m.) motion [12,13] leads to a completely new kind of induced emission [14]. In this way, Scully *et al.* [14] have introduced a new concept called mazer (microwave amplification by the z motion induced emission of radiation). The quantum theory of single mode mazer operating on two-level atoms has been developed in great detail [15–17]. The steady state photon distribution of the mazer operating on two-level atoms under the resonance condition looks similar to a pair of thermal distributions one of which is shifted towards the larger photon number [14]. This state which can be viewed as a mixture of the thermal state and the shifted thermal state, has been shown to be nonclassical [18]. The work of Meyer *et al.* has been extended to treat the theory of single mode two-photon mazer [19]. The interaction between an ultracold Λ-type three-level atom with degenerate ground levels and a single mode radiation field has been studied and the effect of detunings on the photon emission probability of an excited atom has been discussed [20]. In this paper, we examine the two-mode mazer. We follow very closely the work of Meyer, Scully, and Walther [15].

The organization of the paper is as follows. In Sec. II, we study the interaction of three-level cold atoms moving through the two-mode cavity and we show the correlation between the internal dynamics and the external z motion of atoms. In Sec. III, we discuss the transmission of an atom incident on the cavity in various initial states. In Sec. IV, we derive the master equation for the reduced density matrix of the field in the cavity. In Sec. V, the steady state photon probability distribution under the condition of detailed balance is derived. In Sec. VI, the photon statistics of cavity field in a fixed mode has been discussed. In Sec. VII, we obtain the steady state photon probability distribution numerically for the case of unequal coupling constants for the two cavity modes.

II. MODEL SYSTEM AND DYNAMICS

We consider a beam of slow, monoenergetic three-level atoms with a Λ-type configuration passing through a high Q, two-mode microwave cavity of length L. The atomic flux is so adjusted that only one atom interacts with the cavity field at a time. The energy level diagram for the analysis is shown in Fig. 1. The transition between the two lower levels b_1 and b_2 is dipole forbidden and the transition from the upper level a to any of the lower levels b_1 and b_2 is allowed. The frequencies of the transitions $a \rightarrow b_1$ and $a \rightarrow b_2$, coincide with those of the modes 1 and 2 of the microwave cavity so that the atom and the fields interact resonantly. We also neglect

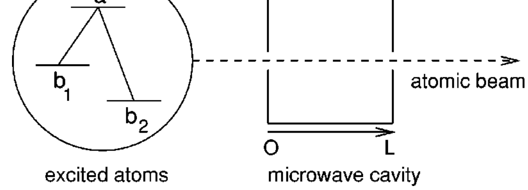

FIG. 1. The scheme of the two-mode micromaser and the energy-level diagram for the analysis.

the cavity field damping during the time an atom interacts with the cavity field. The Hamiltonian for the atom-field interaction including the quantization of the c.m. motion of the atoms, is given by

$$H=H_A+H_F+H_{\mathrm{AF}}. \tag{1}$$

where H_A (H_F) is the Hamiltonian of the free atom (field) and H_{AF} is the interaction Hamiltonian describing the atom-field interaction in the dipole and the rotating wave approximations:

$$H_A=\frac{p_z^2}{2m}+\hbar\Omega_a|a\rangle\langle a|+\sum_{\alpha=1}^{2}\hbar\Omega_{b_\alpha}|b_\alpha\rangle\langle|b_\alpha|,$$

$$H_F=\sum_{\alpha=1}^{2}\hbar\omega_\alpha a_\alpha^\dagger a_\alpha, \tag{2}$$

$$H_{\mathrm{AF}}=\sum_{\alpha=1}^{2}\hbar g_\alpha(a_\alpha|a\rangle\langle b_\alpha|+|b_\alpha\rangle\langle a|a_\alpha^\dagger).$$

The operator $|j\rangle\langle j|(j=a,b_1,b_2)$ gives the projection on to the state $|j\rangle$ with energy $\hbar\Omega_j$. The operators $|i\rangle\langle j|(i,j=a,b_1,b_2;i\neq j)$ describe the transition from level j to level i. The operators a_α ($a_\alpha^\dagger$) annihilate (create) a photon in modes α with the resonance frequencies $\omega_\alpha=\Omega_a-\Omega_{b_\alpha}$. The parameters g_α are the corresponding atom-field coupling constants and m is the atomic mass. The parameters g_α are dependent on z through the mode function of the cavity.

In a suitable reference frame, the Hamiltonian (1) of the atom-field system reads

$$H_I=\frac{p_z^2}{2m}+H_{\mathrm{AF}}. \tag{3}$$

The operator H_{AF} is readily diagonalizable. It has eigenstates $|\phi^0_{n_1+1,n_2+1}\rangle,|\phi^\pm_{n_1+1,n_2+1}\rangle$ with eigenvalues 0, $\pm\hbar\sqrt{g_1^2(n_1+1)+g_2^2(n_2+1)}$, respectively, where

$$|\phi^0_{n_1+1,n_2+1}\rangle=\Bigg[\frac{g_2\sqrt{n_2+1}}{\sqrt{g_1^2(n_1+1)+g_2^2(n_2+1)}}|b_1,n_1+1,n_2\rangle-\frac{g_1\sqrt{n_1+1}}{\sqrt{g_1^2(n_1+1)+g_2^2(n_2+1)}}|b_2,n_1,n_2+1\rangle\Bigg],$$

$$|\phi^\pm_{n_1+1,n_2+1}\rangle=\frac{1}{\sqrt{2}}\Bigg[|a,n_1,n_2\rangle\pm\frac{g_1\sqrt{n_1+1}}{\sqrt{g_1^2(n_1+1)+g_2^2(n_2+1)}}|b_1,n_1+1,n_2\rangle\pm\frac{g_2\sqrt{n_2+1}}{\sqrt{g_1^2(n_1+1)+g_2^2(n_2+1)}}|b_2,n_1,n_2+1\rangle\Bigg]. \tag{4}$$

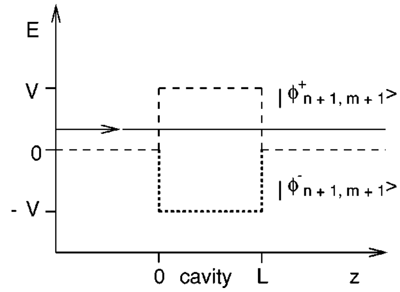

FIG. 2. Schematic representation of the energy E of the excited atoms incident upon a two-mode micromaser cavity with (n,m) photons. The interaction is equivalent to reflection and transmission of atoms through a potential barrier (dashed) or potential well (dotted) with a potential energy $V=\hbar\sqrt{g_1^2(n+1)+g_2^2(m+1)}$. Thus reflection and transmission of the atom is very similar to the one in the work of Meyer *et al.* However, the atom can be reflected and transmitted in either of the three states $|a,n,m\rangle$, $|b_1,n+1,m\rangle$, and $|b_2,n,m+1\rangle$.

In the basis of dressed states $|\phi^\pm_{n_1+1,n_2+1}\rangle$, $|\phi^0_{n_1+1,n_2+1}\rangle$ of the atom-field system, the Hamiltonian (3) leads to

$$H_I|\phi^\pm_{n_1+1,n_2+1}\rangle=h_\pm|\phi^\pm_{n_1+1,n_2+1}\rangle,$$
$$H_I|\phi^0_{n_1+1,n_2+1}\rangle=h_0|\phi^0_{n_1+1,n_2+1}\rangle. \tag{5}$$

Here $h_\pm=p_z^2/2m\pm\hbar\sqrt{g_1^2(z)(n_1+1)+g_2^2(z)(n_2+1)}$ and $h_0=p_z^2/2m$. Note that $h_\pm$ and h_0 are still operators which act in the space of the center of mass variables. If we expand the wave function of the combined atom-cavity system as

$$|\Psi\rangle=\chi_+|\phi^+_{n_1+1,n_2+1}\rangle+\chi_-|\phi^-_{n_1+1,n_2+1}\rangle+\chi_0|\phi^0_{n_1+1,n_2+1}\rangle, \tag{6}$$

then

$$i\hbar\frac{\partial\chi_\alpha}{\partial t}=h_\alpha\chi_\alpha,\quad \alpha=\pm,0. \tag{7}$$

Clearly the effect of the cavity with fixed number of photons in each mode is to produce a potential term in h as discussed in Ref. [12]. If we approximate the mode function of the cavity by a mesa function $g(z)=\theta(z)\theta(L-z)$, then the potential terms will be as displayed in Fig. 2.

We now consider the initial atom-field state to be $|a,n_1,n_2\rangle$, i.e., the atom is in the excited state with n_1 photons in mode 1 and n_2 photons in mode 2 of the cavity field. This state can be expanded in terms of the dressed states (4) as

$$|a,n_1,n_2\rangle=\frac{1}{\sqrt{2}}[|\phi^+_{n_1+1,n_2+1}\rangle+|\phi^-_{n_1+1,n_2+1}\rangle]. \tag{8}$$

From the above discussions, the problem is now reduced to that of an atom incident upon the potentials $V^\pm_{n_1+1,n_2+1}(z)=\pm\hbar\sqrt{g_1^2(n_1+1)+g_2^2(n_2+1)}$. We consider the c.m. wave packet of the incident atom to be $\psi(z,0)$

$=\int d\,kA(k)e^{ikz}\theta(-z)$ where the amplitudes $A(k)$ are adjusted such that the center of wave packet enters the cavity at time $t=0$. The Heaviside's step function $\theta(-z)$ merely limits the spread of the initial wave packet to the $z<0$ region only. The wave function of the atom-field system initially is

$$\langle z|\Psi(0)\rangle=\psi(z,0)|a,n_1,n_2\rangle. \tag{9}$$

By using Eq. (8) the wave function of the atom-field system at time t is found to be

$$\begin{aligned}\langle z|\Psi(t)\rangle&=\exp(-iH_It/\hbar)\,\psi(z,0)|a,n_1,n_2\rangle\\&=\exp(-iH_It/\hbar)\,\psi(z,0)\frac{1}{\sqrt{2}}[|\phi^+_{n_1+1,n_2+1}\rangle+|\phi^-_{n_1+1,n_2+1}\rangle]\\&=\frac{1}{\sqrt{2}}\Bigg[\exp\Bigg(\frac{-it}{\hbar}\Bigg[\frac{p_z^2}{2m}+\hbar\sqrt{g_1^2(n_1+1)+g_2^2(n_2+1)}\Bigg]\Bigg)\psi(z,0)|\phi^+_{n_1+1,n_2+1}\rangle\\&\quad+\exp\Bigg(\frac{-it}{\hbar}\Bigg[\frac{p_z^2}{2m}-\hbar\sqrt{g_1^2(n_1+1)+g_2^2(n_2+1)}\Bigg]\Bigg)\psi(z,0)|\phi^-_{n_1+1,n_2+1}\rangle\Bigg].\end{aligned} \tag{10}$$

Denoting the reflection and transmission amplitudes as $\rho^{\pm}_{n_1,n_2},\tau^{\pm}_{n_1,n_2}$ for the potential barrier-well problem of the dressed states $|\phi^{\pm}_{n_1+1,n_2+1}\rangle$, respectively, we have

$$\rho^{\pm}_{n_1,n_2}=i\Delta^{\pm}_{n_1,n_2}\sin(k^{\pm}_{n_1,n_2}L)\,\tau^{\pm}_{n_1,n_2}, \tag{11}$$

$$\tau^{\pm}_{n_1,n_2}=[\cos(k^{\pm}_{n_1,n_2}L)-i\Sigma^{\pm}_{n_1,n_2}\sin(k^{\pm}_{n_1,n_2}L)]^{-1}, \tag{12}$$

$$\Delta^{\pm}_{n_1,n_2}=\frac{1}{2}\left(\frac{k^{\pm}_{n_1,n_2}}{k}-\frac{k}{k^{\pm}_{n_1,n_2}}\right), \tag{13}$$

$$\Sigma^{\pm}_{n_1,n_2}=\frac{1}{2}\left(\frac{k^{\pm}_{n_1,n_2}}{k}+\frac{k}{k^{\pm}_{n_1,n_2}}\right),$$

$$\begin{aligned}k^{\pm}_{n_1,n_2}&=\sqrt{\left(k^2\mp\frac{2m}{\hbar}\sqrt{g_1^2(n_1+1)+g_2^2(n_2+1)}\right)}\\&=\sqrt{\left(k^2\mp\kappa^2\sqrt{\frac{g_1^2(n_1+1)+g_2^2(n_2+1)}{g_1^2+g_2^2}}\right)},\end{aligned} \tag{14}$$

where $\hbar k$ is the atomic c.m. momentum and $\hbar^2\kappa^2/2m=\hbar\sqrt{g_1^2+g_2^2}$ is the vacuum coupling energy. Carrying out the time evolution of the state ket in Eq. (10) for the potential barrier-well problem of the dressed states, we obtain the following wave function of the atom-field system after the atom has left the interaction region

$$\begin{aligned}\langle z|\Psi(t)\rangle=\int dkA(k)e^{-i(\hbar k^2/2m)t}\{&[R_{a,n_1,n_2}(k)e^{-ikz}\theta(-z)\\&+T_{a,n_1,n_2}(k)e^{ik(z-L)}\theta(z-L)]|a,n_1,n_2\rangle\\&+[R_{b_1,n_1+1,n_2}(k)e^{-ikz}\theta(-z)\\&+T_{b_1,n_1+1,n_2}(k)e^{ik(z-L)}\theta(z-L)]|b_1,n_1+1,n_2\rangle\\&+[R_{b_2,n_1,n_2+1}(k)e^{-ikz}\theta(-z)\\&+T_{b_2,n_1,n_2+1}(k)e^{ik(z-L)}\theta(z-L)]\\&\times|b_2,n_1,n_2+1\rangle\},\end{aligned} \tag{15}$$

where

$$R_{a,n_1,n_2}=\frac{1}{2}(\rho^+_{n_1,n_2}+\rho^-_{n_1,n_2}),\ T_{a,n_1,n_2}=\frac{1}{2}(\tau^+_{n_1,n_2}+\tau^-_{n_1,n_2}), \tag{16}$$

are the probability amplitudes that the atom is reflected or transmitted with the atom-field state remaining in the same initial state as $|a,n_1,n_2\rangle$ and

$$R_{b_1,n_1+1,n_2}=\frac{g_1\sqrt{n_1+1}}{2\sqrt{g_1^2(n_1+1)+g_2^2(n_2+1)}}(\rho^+_{n_1,n_2}-\rho^-_{n_1,n_2})$$

$$\begin{aligned}T_{b_1,n_1+1,n_2}=&\frac{g_1\sqrt{n_1+1}}{2\sqrt{g_1^2(n_1+1)+g_2^2(n_2+1)}}\\&\times(\tau^+_{n_1,n_2}-\tau^-_{n_1,n_2}),\end{aligned} \tag{17}$$

are the probability amplitudes that the atom is reflected or transmitted when the atom-field state makes a transition from initial $|a,n_1,n_2\rangle$ to $|b_1,n_1+1,n_2\rangle$. Similarly, the atom is reflected or transmitted when the atom-field state changes to $|b_2,n_1,n_2+1\rangle$ with amplitudes

$$R_{b_2,n_1,n_2+1}=\frac{g_2\sqrt{n_2+1}}{2\sqrt{g_1^2(n_1+1)+g_2^2(n_2+1)}}(\rho^+_{n_1,n_2}-\rho^-_{n_1,n_2}),$$

$$T_{b_2,n_1,n_2+1}=\frac{g_2\sqrt{n_2+1}}{2\sqrt{g_1^2(n_1+1)+g_2^2(n_2+1)}}\times(\tau^+_{n_1,n_2}-\tau^-_{n_1,n_2}). \quad (18)$$

Note that all the physical characteristics regarding the interaction of ultracold atoms with a high quality cavity can be calculated in terms of quantities defined by Eqs. (16)–(18). Let us examine the probability of emission of a photon. When an initially excited three-level atom is incident upon the cavity containing (n_1,n_2) photons in the two modes (1,2), respectively, then from Eqs. (17) and (18) the probability that the atom goes to the level b_1 and emits a photon in mode 1 is

$$p_{(n_1,n_2)}(a\rightarrow b_1)=|R_{b_1,n_1+1,n_2}|^2+|T_{b_1,n_1+1,n_2}|^2, \quad (19)$$

the probability that the atom goes to the level b_2 and emits a photon in mode 2 is

$$p_{(n_1,n_2)}(a\rightarrow b_2)=|R_{b_2,n_1,n_2+1}|^2+|T_{b_2,n_1,n_2+1}|^2, \quad (20)$$

and the probability that the atom emits a photon either in mode 1 (or) mode 2 inside the cavity is

$$p_{(n_1,n_2)}(\text{emission})=|R_{b_1,n_1+1,n_2}|^2+|T_{b_1,n_1+1,n_2}|^2+|R_{b_2,n_1,n_2+1}|^2+|T_{b_2,n_1,n_2+1}|^2. \quad (21)$$

III. TRANSMISSION OF ATOMS

In this section, we discuss the transmission characteristics of an ultracold atom through the cavity induced potentials. In the previous section, we have seen that for an incident atom in the excited state, the two orthogonal dressed states $|\phi^\pm_{n_1+1,n_2+1}\rangle$ create barrier-well potentials for the external motion of atoms. When the initial atom-field state is $|a,0,0\rangle$, the probability of transmission in the excited state of an atom through the cavity is plotted as a function of κL in Fig. 3(a) by using Eq. (16) for the parameter $k/\kappa=0.01$. The graph shows resonances at $\kappa L=m\pi$ with $m=1,2,\ldots$, which is similar to the transmission of an excited two-level atom incident on a single mode cavity [15]. As described in Ref. [15], this feature is just the transmission characteristic of the potential well.

Next we consider the initial atom-field state to be either $|b_1,1,0\rangle$ or $|b_2,0,1\rangle$. Using the same procedure as in the previous section, we obtain the time evolution for the initial state $|b_1,1,0\rangle$. Here it is important to note that the dressed state $|\phi^0_{n_1,n_2}\rangle$ also contributes since

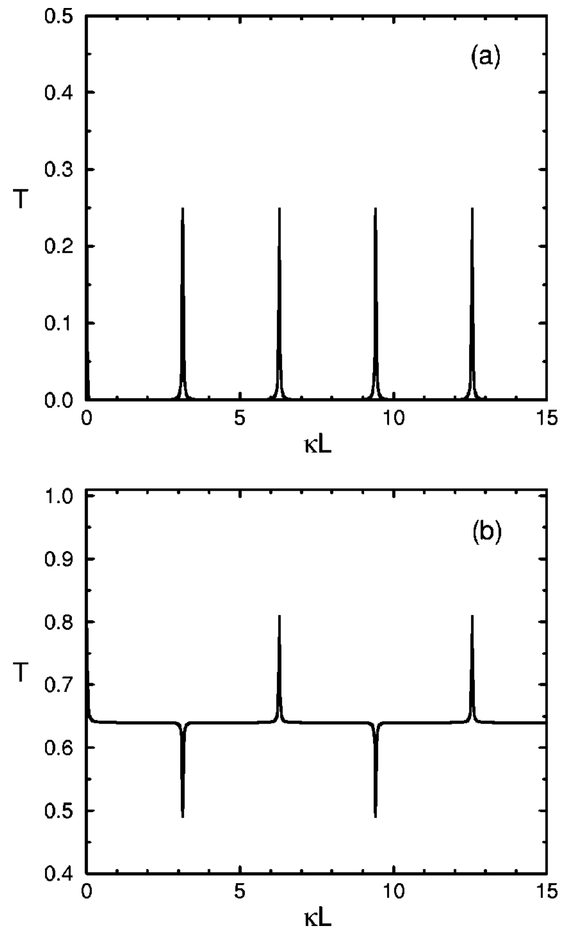

FIG. 3. The probability of transmission T of an atom in the initial state through the cavity as a function of the length of the cavity κL for the parameters $g_2/g_1=2$, $k/\kappa=0.01$ and for the initial atom-field states (a) $|a,0,0\rangle$ $(T\equiv|T_{a,0,0}|^2)$ and (b) $|b_1,1,0\rangle$ $(T\equiv|T_{b_1,1,0}|^2)$. For the initial atom-field state $|a,0,0\rangle$, the probability of transmission is independent of the ratio g_2/g_1.

$$|b_1,1,0\rangle=\frac{g_2}{\sqrt{g_1^2+g_2^2}}|\phi^0_{1,1}\rangle+\frac{g_1}{\sqrt{2(g_1^2+g_2^2)}}(|\phi^+_{1,1}\rangle-|\phi^-_{1,1}\rangle). \quad (22)$$

A repeat of steps (9)–(16) now yields the probability T that an atom is transmitted in the same initial state

$$T=|T_{b_1,1,0}|^2=\left|\frac{g_1^2}{2(g_1^2+g_2^2)}(\tau^+_{0,0}+\tau^-_{0,0})+\frac{g_2^2}{(g_1^2+g_2^2)}\right|^2, \quad (23)$$

where $\tau^\pm_{0,0}$ are given by Eq. (12) and the additional factor of $g_2^2/(g_1^2+g_2^2)$ comes from the contribution due to the dressed state $|\phi^0_{n_1,n_2}\rangle$ in the expansion (22). Using Eq. (23), the transmission probability that an atom in the initial state $|b_1\rangle$ is transmitted through the cavity containing initially one photon in mode 1 has been plotted in Fig. 3(b) for the parameters $g_2/g_1=2$, $k/\kappa=0.01$. On comparing the graphs 3(a) and 3(b), we see that the effect of the dark state $|\phi^0_{n_1,n_2}\rangle$ enhances the probability of transmission of atom in the initial state $|b_1\rangle$ at $\kappa L = m\pi$ with $m = 2,4,6, \ldots$. We also see that we have the possibility of determining the phase $\theta_{a,0,0}$ of the amplitude $\frac{1}{2}(\tau_{0,0}^{+} + \tau_{0,0}^{-}) \equiv T_{a,0,0}$ from the measurements of $T_{a,0,0}$ and $T_{b_1,1,0}$:

$$|T_{b_1,1,0}|^2 \equiv \frac{1}{(g_1^2+g_2^2)^2}[g_1^4|T_{a,0,0}|^2 + g_2^4 + 2g_1^2g_2^2|T_{a,0,0}|\cos(\theta_{a,0,0})]. \tag{24}$$

Note that Fig. 3(a) yields $|T_{a,0,0}|^2$ and Fig. 3(b) gives $|T_{b_1,1,0}|^2$. Clearly from these two figures one can get $\theta_{a,0,0}$. This has become possible due to the interference between the contributions coming from different dressed states in the expansion (22).

IV. BUILDUP OF THE CAVITY FIELD

In this section, we derive the master equation for the cavity field assuming that a steady atomic beam passes through the cavity. The successive passage of atoms changes the field in the cavity. In the analysis of Sec. II, we had assumed the cavity field to be in the Fock state. However, for the dynamic evolution of the field we have to examine a more general initial state of the cavity field. Using Eq. (8) the wave function of the initial atom-field system is now given by

$$\begin{aligned}\langle z|\Psi(0)\rangle &= \psi(z,0)\sum_{n_1,n_2} C_{n_1,n_2}|a,n_1,n_2\rangle \\ &= \psi(z,0)\frac{1}{\sqrt{2}}\sum_{n_1,n_2} C_{n_1,n_2}(|\phi^{+}_{n_1+1,n_2+1}\rangle \\ &\quad + |\phi^{-}_{n_1+1,n_2+1}\rangle).\end{aligned} \tag{25}$$

Carrying out the time evolution for this initial state using Eq. (15), the state of atom-field system after the interaction is given by

$$\begin{aligned}\langle z|\Psi(t)\rangle = \int dk A(k)e^{-i(\hbar k^2/2m)t}\sum_{n_1,n_2=0}^{\infty}[&\mathcal{R}_{a,n_1,n_2}(k)e^{-ikz}\theta(-z)|a,n_1,n_2\rangle + \mathcal{T}_{a,n_1,n_2}(k)e^{ik(z-L)}\theta(z-L)|a,n_1,n_2\rangle \\ &+ \mathcal{R}_{b_1,n_1+1,n_2}(k)e^{-ikz}\theta(-z)|b_1,n_1+1,n_2\rangle + \mathcal{T}_{b_1,n_1+1,n_2}(k)e^{ik(z-L)}\theta(z-L)|b_1,n_1+1,n_2\rangle \\ &+ \mathcal{R}_{b_2,n_1,n_2+1}(k)e^{-ikz}\theta(-z)|b_2,n_1,n_2+1\rangle + \mathcal{T}_{b_2,n_1,n_2+1}(k)e^{ik(z-L)}\theta(z-L)|b_2,n_1,n_2+1\rangle],\end{aligned} \tag{26}$$

where

$$\begin{aligned}\mathcal{R}_{a,n_1,n_2}(k) &= C_{n_1,n_2}R_{a,n_1,n_2}(k), \\ \mathcal{T}_{a,n_1,n_2}(k) &= C_{n_1,n_2}T_{a,n_1,n_2}(k),\end{aligned} \tag{27}$$

are the probability amplitudes for reflection (or) transmission of the atom in the upper state $|a\rangle$ with the cavity field containing (n_1,n_2) photons in the two modes and similarly, the atom is reflected (or) transmitted when the atom-field state is $|b_1,n_1+1,n_2\rangle$ (or) $|b_2,n_1,n_2+1\rangle$ with amplitudes

$$\begin{aligned}\mathcal{R}_{b_1,n_1+1,n_2}(k) &= C_{n_1,n_2}R_{b_1,n_1+1,n_2}(k), \\ \mathcal{T}_{b_1,n_1+1,n_2}(k) &= C_{n_1,n_2}T_{b_1,n_1+1,n_2}(k), \\ \mathcal{R}_{b_2,n_1,n_2+1}(k) &= C_{n_1,n_2}R_{b_2,n_1,n_2+1}(k), \\ \mathcal{T}_{b_2,n_1,n_2+1}(k) &= C_{n_1,n_2}T_{b_2,n_1,n_2+1}(k).\end{aligned} \tag{28}$$

Equation (26) can be used to find the atom-field density matrix after a single atom has passed through the cavity. By taking the trace over the atomic energy eigenstates and the position eigenstates of the center of mass of the atom, the reduced density operator $\rho(t)$ of the cavity field is then found to be

$$\rho(t) = \sum_{i=a,b_1,b_2}\int dz\langle i,z|\Psi(t)\rangle\langle\Psi(t)|i,z\rangle. \tag{29}$$

We consider the case in which excited atoms are injected into the cavity at random times and the time interval between successive atoms entering the cavity obeys a Poissonian distribution with an average r. As discussed in Ref. [4], the contribution of each atom passing through the cavity and the field damping lead to the following coarse grained time evolution of reduced density operator of the field in the interaction picture:

$$\dot{\rho}(t) = r\,\delta\rho(t) + L\rho(t), \tag{30}$$

where $\delta\rho(t)$ is the change in $\rho(t)$ due to the passage of a single atom in the excited state. The field damping and the effect of thermal photons are described by the Liouville operator

$$\begin{aligned}L\rho = &\frac{1}{2}C_1(n_{b_1}+1)(2a_1\rho a_1^{\dagger} - a_1^{\dagger}a_1\rho - \rho a_1^{\dagger}a_1) \\ &+ \frac{1}{2}C_1 n_{b_1}(2a_1^{\dagger}\rho a_1 - a_1a_1^{\dagger}\rho - \rho a_1a_1^{\dagger}) \\ &+ \frac{1}{2}C_2(n_{b_2}+1)(2a_2\rho a_2^{\dagger} - a_2^{\dagger}a_2\rho - \rho a_2^{\dagger}a_2) \\ &+ \frac{1}{2}C_2 n_{b_2}(2a_2^{\dagger}\rho a_2 - a_2a_2^{\dagger}\rho - \rho a_2a_2^{\dagger}).\end{aligned} \tag{31}$$

Here n_{b_α} is the number of thermal photons in mode α and C_α is the damping rate of this mode. Using Eqs. (29)–(31) we obtain the equation governing the time evolution of the density matrix elements

$$\begin{aligned}\dot{\rho}(n_1,n_2;n_1',n_2') = r\{ & (R_{a,n_1,n_2}R^\star_{a,n_1',n_2'} + T_{a,n_1,n_2}T^\star_{a,n_1',n_2'} - 1)\rho(n_1,n_2;n_1',n_2') \\ & + (R_{b_1,n_1,n_2}R^\star_{b_1,n_1',n_2'} + T_{b_1,n_1,n_2}T^\star_{b_1,n_1',n_2'})\rho(n_1-1,n_2;n_1'-1,n_2') \\ & + (R_{b_2,n_1,n_2}R^\star_{b_2,n_1',n_2'} + T_{b_2,n_1,n_2}T^\star_{b_2,n_1',n_2'})\rho(n_1,n_2-1;n_1',n_2'-1)\} + \frac{1}{2}C_1(n_{b_1}+1) \\ & \times[2\sqrt{(n_1+1)(n_1'+1)}\rho(n_1+1,n_2;n_1'+1,n_2') - (n_1+n_1')\rho(n_1,n_2;n_1',n_2')] \\ & + \frac{1}{2}C_1 n_{b_1}[2\sqrt{n_1 n_1'}\rho(n_1-1,n_2;n_1'-1,n_2') - (n_1+n_1'+2)\rho(n_1,n_2;n_1',n_2')] + \frac{1}{2}C_2(n_{b_2}+1) \\ & \times[2\sqrt{(n_2+1)(n_2'+1)}\rho(n_1,n_2+1;n_1',n_2'+1) - (n_2+n_2') \\ & \times\rho(n_1,n_2;n_1',n_2')] + \frac{1}{2}C_2 n_{b_2}[2\sqrt{n_2 n_2'}\rho(n_1,n_2-1;n_1',n_2'-1) - (n_2+n_2'+2)\rho(n_1,n_2;n_1',n_2')].\end{aligned} \tag{32}$$

The diagonal elements of the density matrix $P(n_1,n_2)=\rho(n_1,n_2;n_1,n_2)$ which gives the joint distribution of photons in the two cavity modes, obeys the equation

$$\begin{aligned}\dot{P}(n_1,n_2) = r\{ & [|R_{a,n_1,n_2}|^2 + |T_{a,n_1,n_2}|^2 - 1]P(n_1,n_2) + [|R_{b_1,n_1,n_2}|^2 + |T_{b_1,n_1,n_2}|^2]P(n_1-1,n_2) \\ & + [|R_{b_2,n_1,n_2}|^2] + |T_{b_2,n_1,n_2}|^2]P(n_1,n_2-1)\} + C_1(n_{b_1}+1)[(n_1+1)P(n_1+1,n_2) - n_1 P(n_1,n_2)] \\ & + C_1 n_{b_1}[n_1 P(n_1-1,n_2) - (n_1+1)P(n_1,n_2)] \\ & + C_2(n_{b_2}+1)[(n_2+1)P(n_1,n_2+1) - n_2 P(n_1,n_2) \\ & + C_2 n_{b_2}[n_2 P(n_1,n_2-1) - (n_2+1)P(n_1,n_2)].\end{aligned} \tag{33}$$

This is the master equation for the two-mode micromaser. This equation has the character of rate equation for the probability and various terms on the right hand side behave as the outflow and the inflow of probabilities. This equation has also the form that one would have expected on physical grounds.

V. ANALYTICAL SOLUTION OF MASTER EQUATION

The steady state photon probability distribution is obtained by setting

$$\dot{P}(n_1,n_2)=0. \tag{34}$$

The distribution $P(n_1,n_2)$ can be obtained in analytical form by using the condition of detailed balance which states that the net inflow and outflow of probabilities are equal. This leads to

$$P(n_1,n_2)=P(n_1-1,n_2)\frac{1}{C_1(n_{b_1}+1)}\left\{C_1 n_{b_1}+\frac{G_{b_1,n_1-1,n_2}}{n_1}\right\}, \tag{35}$$

$$P(n_1,n_2)=P(n_1,n_2-1)\frac{1}{C_2(n_{b_2}+1)}\times\left\{C_2 n_{b_2}+\frac{G_{b_2,n_1,n_2-1}}{n_2}\right\}. \tag{36}$$

Here $G_{b_1,n_1-1,n_2}=r\ p_{(n_1-1,n_2)}(a\to b_1)$, $G_{b_2,n_1,n_2-1}=r\ p_{(n_1,n_2-1)}(a\to b_2)$ are the gain coefficients for modes 1 and 2, respectively, with $p_{(n_1,n_2)}(a\to b_1)$, $p_{(n_1,n_2)}(a\to b_2)$ as defined in Eqs. (19) and (20). Substituting the expression for $P(n_1-1,n_2)$ obtained from Eq. (36) into Eq. (35) and the expression for $P(n_1,n_2-1)$ obtained from Eq. (35) into Eq. (36), we get

$$\begin{aligned}P(n_1,n_2)=P(n_1-1,n_2-1)&\frac{1}{C_1(n_{b_1}+1)}\frac{1}{C_2(n_{b_2}+1)} \\ &\times\left(C_1 n_{b_1}+\frac{G_{b_1,n_1-1,n_2}}{n_1}\right) \\ &\times\left(C_2 n_{b_2}+\frac{G_{b_2,n_1-1,n_2-1}}{n_2}\right),\end{aligned} \tag{37}$$

$$P(n_1,n_2)=P(n_1-1,n_2-1)\frac{1}{C_1(n_{b_1}+1)}\frac{1}{C_2(n_{b_2}+1)}\times\left(C_2n_{b_2}+\frac{G_{b_2,n_1,n_2-1}}{n_2}\right)\times\left(C_1n_{b_1}+\frac{G_{b_1,n_1-1,n_2-1}}{n_1}\right). \quad (38)$$

It is obvious that Eqs. (37) and (38) can both be satisfied if

$$g_1=g_2=g,\quad C_1n_{b_1}=C_2n_{b_2}=Cn_b. \quad (39)$$

Under these conditions, the steady state photon distribution has the form

$$P(n_1,n_2)=P(0,0)\left(\frac{r}{C_1+Cn_b}\right)^{n_1}\left(\frac{r}{C_2+Cn_b}\right)^{n_2}\times\prod_{q=1}^{n_1+n_2}\left\{\frac{Cn_b}{r}+\frac{1}{2(q+1)}\left[1-\frac{(1+\Delta_q^+\Delta_q^-S_q^+S_q^-)(C_q^+C_q^-+\Sigma_q^+\Sigma_q^-S_q^+S_q^-)}{(C_q^{+2}+\Sigma_q^{+2}S_q^{+2})(C_q^{-2}+\Sigma_q^{-2}S_q^{-2})}\right]\right\}, \quad (40)$$

where $C_q^{\pm}=\cos(k_q^{\pm}L)$, $S_q^{\pm}=\sin(k_q^{\pm}L)$ with $k_q^{\pm}=\sqrt{(k^2\mp\kappa^2\sqrt{(q+1)/2})}$ which is the same as Eq. (14) of Sec. II with (n_1+n_2+1) replaced by q and $g_1=g_2=g$. Similarly $\Delta_q^{\pm},\Sigma_q^{\pm}$ are defined by Eqs. (13) with $k_{n_1,n_2}^{\pm}$ replaced by $k_q^{\pm}$. The normalization condition of joint probability gives $\Sigma_{n_1,n_2=0}^{\infty}P(n_1,n_2)=1$. The expression (40) contains all the statistical information about the steady state field. We consider the special case in which all the parameters for the two modes are equal, i.e., $g_1=g_2=g$, $C_1=C_2=C$, $n_{b_1}=n_{b_2}=n_b$. In this case, Eq. (39) can be satisfied and the detailed balance steady state photon distribution has the form

$$P(n_1,n_2)=f(n_1+n_2), \quad (41)$$

where

$$f(n)=P(0,0)\left[\frac{r}{C(n_b+1)}\right]^n\prod_{q=1}^{n}\left\{\frac{Cn_b}{r}+\frac{1}{(q+1)}\left[\frac{1}{2}\left(1-\frac{(1+\Delta_q^+\Delta_q^-S_q^+S_q^-)(C_q^+C_q^-+\Sigma_q^+\Sigma_q^-S_q^+S_q^-)}{(C_q^{+2}+\Sigma_q^{+2}S_q^{+2})(C_q^{-2}+\Sigma_q^{-2}S_q^{-2})}\right)\right]\right\}. \quad (42)$$

It is to be noted that the square bracketted term inside the product in the above equation, is identical to the photon emission probability of an ultracold, excited two-level atom entering a single mode resonant cavity containing q photons in the single mode mazer [15]. For comparison the steady state photon distribution of the single mode mazer operating on two-level atoms with the atom-field coupling constant g [15] is

$$P(n)=P(0)\left[\frac{r}{C(n_b+1)}\right]^n\prod_{q=1}^{n}\left\{\frac{Cn_b}{r}+\frac{p_e(q-1)}{q}\right\}. \quad (43)$$

Here $p_e(q)$ is the photon emission probability of an excited atom incident on the cavity containing q photons and is equal to the square bracketted term in Eq. (42) with g replaced by $g/\sqrt{2}$. For fast atoms, i.e., when the energy of incident atoms is very large compared to the vacuum coupling energy, the square bracketed term in Eq. (42) can be approximated to $\sin^2(g\tau\sqrt{q+1})$ (see Sec. V of Ref. [15]) where $g\tau=\kappa^2L/2\sqrt{2}k$. In this case $f(n)$ has the form

$$f(n)=P(0,0)\left[\frac{r}{C(n_b+1)}\right]^n\times\prod_{q=1}^{n}\left\{\frac{Cn_b}{r}+\frac{1}{q+1}\sin^2(g\tau\sqrt{q+1})\right\}, \quad (44)$$

which is the same as obtained in the two-mode micromaser operating on three-level atoms [10]. As mentioned in Ref. [10], $f(n)=P(n,0)=P(0,n)$ is the joint probability of having n photons in one mode and no photons in the other mode and the probability that the cavity contains $'n'$ total number of photons is

$$P_\Sigma(n)\equiv\sum_{n_1+n_2=n}P(n_1,n_2)=f(n)(n+1). \quad (45)$$

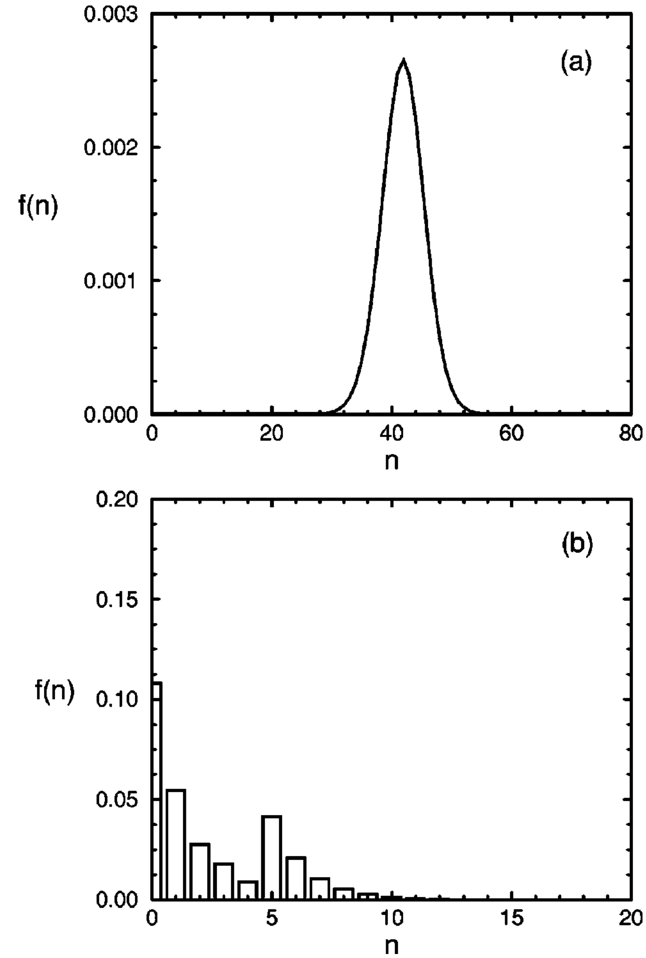

FIG. 4. The function $f(n)=P(n,0)=P(0,n)$ for the parameters $g_1=g_2=g$, $C_1=C_2=C$, $n_{b_1}=n_{b_2}=n_b$, $r/C=100$, $n_b=1$, $\kappa L=10\pi/\sqrt[4]{3}$ and (a) $k/\kappa=10$, (b) $k/\kappa=0.01$.

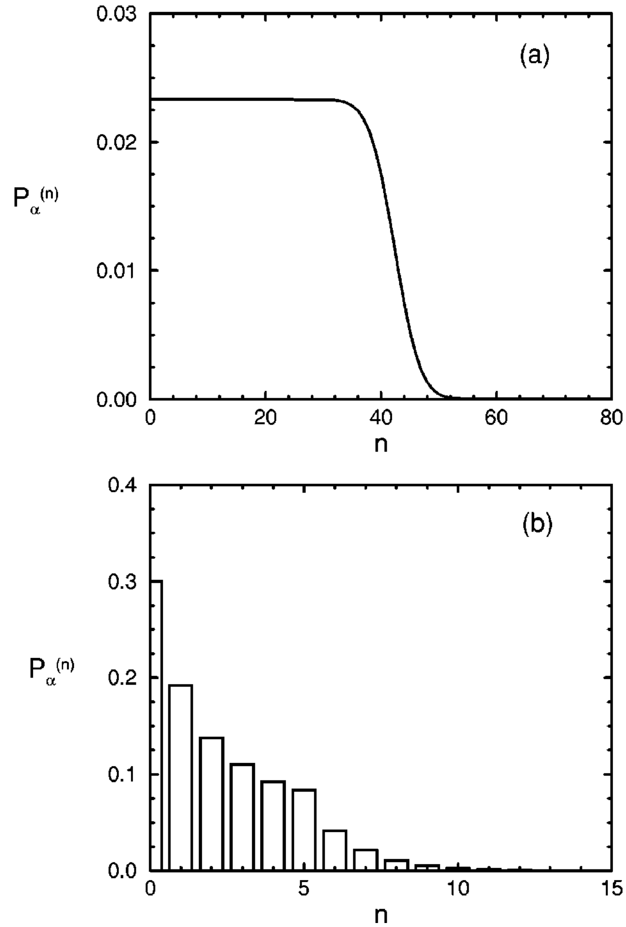

FIG. 5. The distribution of photons in mode α for the parameters $g_1=g_2=g$, $C_1=C_2=C$, $n_{b_1}=n_{b_2}=n_b$, $r/C=100$, $n_b=1$, $\kappa L=10\pi/\sqrt[4]{3}$ and (a) $k/\kappa=10$, (b) $k/\kappa=0.01$.

$P(0,0)$ can be determined from the normalization condition $\sum_{n=0}^{\infty}P_\Sigma(n)=1$. For fast atoms, the graph of $f(n)$ has been plotted in Fig. 4(a) for the parameters $r/C=100$, $n_b=1$, $\kappa L=10\pi/\sqrt[4]{3}$, $k/\kappa=10$. The graph shows the distribution $f(n)$ with single peak and compares well with the Ref. [10] on two-mode micromaser. In general, the function $f(n)$ can have more than one peak depending on the value of $g\tau=\kappa^2L/2\sqrt{2}k$. The joint probability distribution $f(n)$ behaves differently when the micromaser is pumped by ultracold atoms, i.e., when the energy of incident atoms is very low compared to vacuum coupling energy. For ultracold atoms, $f(n)$ is shown in Fig. 4(b) for the parameters $r/C=100$, $n_b=1$, $\kappa L=10\pi/\sqrt[4]{3}$, $k/\kappa=0.01$. The graph looks similar to a pair of thermal distributions one of which is shifted towards the larger photon number. This behavior of $f(n)$ occurs at $\kappa L=m\pi/\sqrt[4]{N}$ with $m=1,2,\ldots,$ $N=1,\frac{3}{2},2,\ldots,$ and is similar to that of the steady state photon distribution of the single mode mazer [15] as expected on comparing Eqs. (42) and (43). When $\kappa L\neq m\pi/\sqrt[4]{N}$, the distribution $f(n)$ is a decreasing function of *n* similar to a thermal distribution for ultracold incident atoms.

VI. STEADY-STATE PHOTON STATISTICS

From the joint probability distribution $P(n_1,n_2)$, we can obtain the distribution of photons $P_\alpha(n)$ in any fixed mode α by summing over the number of photons in the other mode. The function $P_\alpha(n)$ is defined by

$$P_1(n)=\sum_{l=0}^{\infty} P(n,l), \quad P_2(n)=\sum_{l=0}^{\infty} P(l,n). \tag{46}$$

By using Eq. (41) the function $P_\alpha(n)$ is found to be

$$P_\alpha(n)=\sum_{l=n}^{\infty} f(l). \tag{47}$$

It may be noted from this equation that $P_\alpha(n)$ is independent of α since we assumed $g_1=g_2=g$, $C_1=C_2=C$, $n_{b_1}=n_{b_2}=n_b$, and

$$P_\alpha(n+1)=P_\alpha(n)-f(n). \tag{48}$$

The function $f(n)$ is positive as seen from Eq. (42). Therefore, the photon distribution decreases monotonously with *n*. The probability distribution of photons in a fixed mode cal-

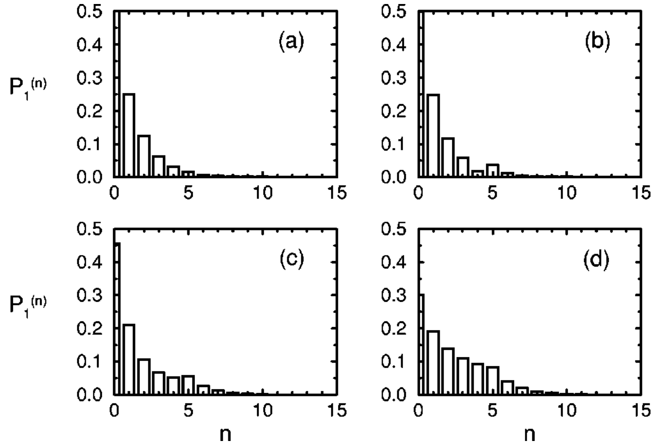

FIG. 6. The distribution of photons in mode 1 at different times t during the evolution from the initial state. Mode 1 is initially in a thermal state with $\langle n_1\rangle = 1$. Mode 2 is initially in the vacuum state. The parameters for the calculations are $g_1 = g_2 = g$, $C_1 = C_2 = C$, $n_{b_1} = n_{b_2} = n_b$, $r/C = 100$, $n_b = 1$, $\kappa L = 10\pi/\sqrt[4]{3}$, $k/\kappa = 0.01$. Graphs (a), (b), (c), and (d) correspond to $t = 0$, $t = 0.1/C$, $t = 1/C$, and $t = 10/C$, respectively.

culated from (47), is plotted both for fast atoms ($k/\kappa = 10$) and ultracold atoms ($k/\kappa = 0.01$) in Fig. 5 for the parameters $r/C = 100$, $n_b = 1$, $\kappa L = 10\pi/\sqrt[4]{3}$. The graphs show that for ultracold atoms there is a steep decrease in the curve of $P_\alpha(n)$ at the value $n = 5$ for the chosen parameters. From Eq. (47), it is clear that this decrease in the curve is due to the two-peaked nature of $f(n)$ behaving similar to a pair of thermal distributions for ultracold incident atoms. We can examine numerically the stability and uniqueness of this steady state result derived under the condition of detailed balance. Using the fourth order Runge kutta method for direct integration of rate equation (33), we have plotted the photon probability distribution in Figs. 6 and 7 at different times for the equal parameter case when the initial state of

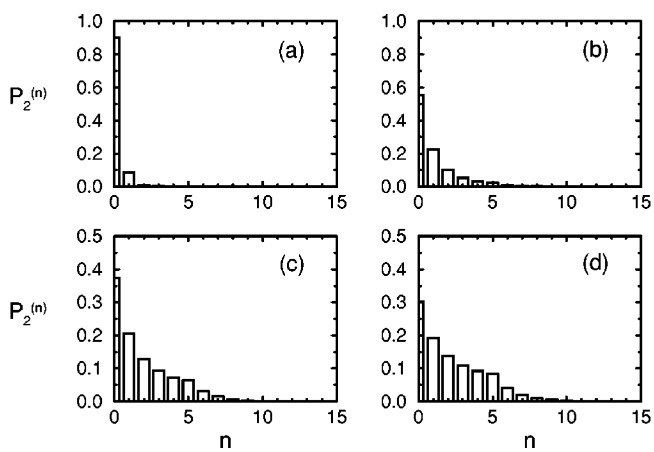

FIG. 7. The distribution of photons in mode 2 at different times t during the evolution from the initial state. Mode 2 is initially in the vacuum state. Mode 1 is initially in a thermal state with $\langle n_1\rangle = 1$. The parameters for the calculations are same as in Fig. 6. Graphs (a), (b), (c), and (d) correspond to $t = 0.1/C$, $t = 1/C$, $t = 3/C$, and $t = 10/C$, respectively.

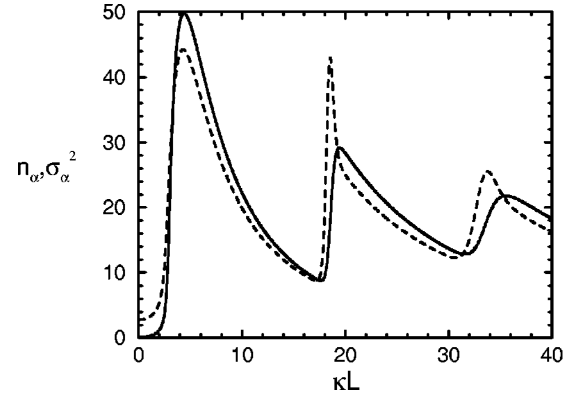

FIG. 8. The mean (solid curve) and the normalized variance (dashed curve) of the distribution of photons in mode α as functions of the interaction length κL for the parameters $r/C = 100$, $n_b = 0.1$, $k/\kappa = 10$. Actual values of σ_α^2 are 0.4 times those shown.

the field for mode 1 is a thermal distribution with the mean value of photon number $\langle n_1\rangle = 1$ and vacuum state for mode 2, for the parameters $r/C = 100$, $n_b = 1$, $\kappa L = 10\pi/\sqrt[4]{3}$, $k/\kappa = 0.01$. It is seen from the graphs that a steady state is reached within a time of order $10/C$ and the steady state photon probability distribution coincides with the analytical result obtained under the principle of detailed balance. This confirms the uniqueness and stability of detailed balance steady state solution.

From Eqs. (42) and (47), we can calculate the first and second moments of the photon distribution in any fixed mode α. From Eq. (47), we find

$$\langle n_\alpha\rangle \equiv \sum_{n=0}^{\infty} nP_\alpha(n) = \frac{1}{2}\sum_{m=0}^{\infty} f(m)m(m+1), \qquad (49)$$

$$\langle n_\alpha^2\rangle \equiv \sum_{n=0}^{\infty} n^2 P_\alpha(n) = \frac{1}{6}\sum_{m=0}^{\infty} f(m)m(m+1)(2m+1). \qquad (50)$$

The mean value of total photon number is found from Eqs. (45) and (49) to be

$$\langle n_\Sigma\rangle \equiv \sum_{n=0}^{\infty} nP_\Sigma(n) = \sum_{n=0}^{\infty} nf(n)(n+1) = 2\langle n_\alpha\rangle \qquad (51)$$

The normalized standard deviation σ_α is defined by

$$\sigma_\alpha^2 = \frac{\langle n_\alpha^2\rangle - \langle n_\alpha\rangle^2}{\langle n_\alpha\rangle}. \qquad (52)$$

In Figs. 8 and 9, we plot the steady-state mean and normalized variance of the distribution of photons in any fixed mode for $r/C = 100$ and $n_b = 0.1$ when the micromaser is pumped by fast and cold atoms. For the case of fast atoms ($k/\kappa = 10$), each mode of the cavity field exhibits features similar to that of the single mode micromaser and the statistics of photons is super-Poissonian ($\sigma_\alpha^2 > 1$). For the case of ultracold atoms ($k/\kappa = 0.01$) the graphs show sharp resonances at $\kappa L = m\pi/\sqrt[4]{N}$ with $m = 1,2,\ldots,$ and N

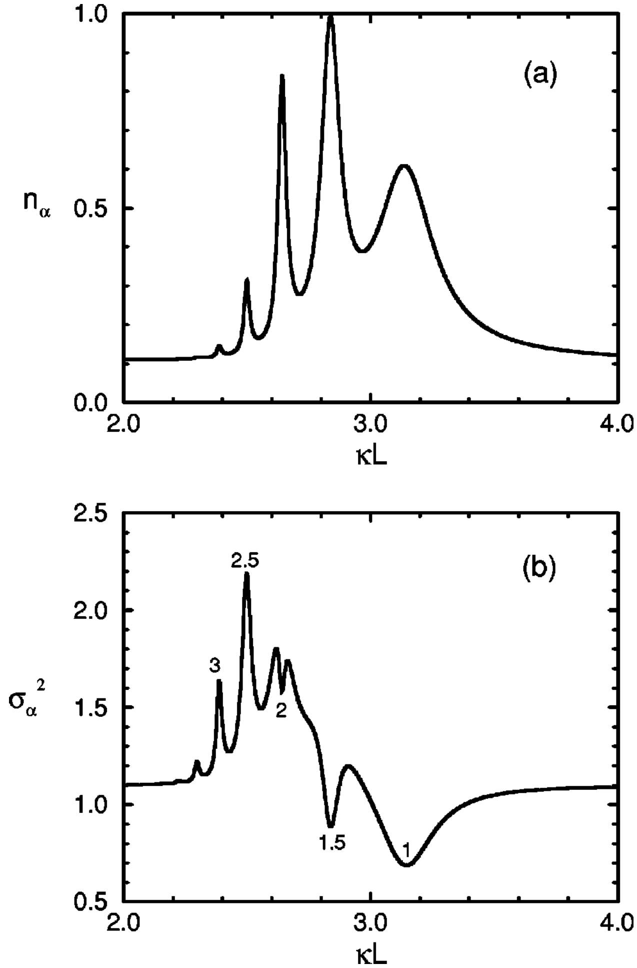

FIG. 9. The mean and the normalized variance of the distribution of photons in mode α as functions of the interaction length κL for the same parameters of Fig. 8 with $k/\kappa=0.01$. The graphs show resonances at $\kappa L=m\pi/\sqrt[4]{N}$. The resonance sequence corresponding to $m=1$ has been plotted and the peaks are labeled by N values.

$=1,\frac{3}{2},2,\ldots$. The peaks in the normalized variance are accompanied by resonances in the mean photon number and are reminiscent of the behavior of single mode mazer [15]. For small values of N, the normalized variance σ_α^2 is less than unity which shows that the photon statistics in each mode is sub-Poissonian. This is because the joint probability function $f(n)$ behaves as a shifted thermal distribution at those resonance positions. Shifting the thermal distribution of $f(n)$ to smaller values of N does not increase the variance of probability distribution $P_\alpha(n)$ when n_b is small. However, the normalized variance σ_α^2 decreases below the Poissonian level because the mean value $\langle n_\alpha\rangle$ is increased. These resonances in the mean value $\langle n_\alpha\rangle$ give rise to a strong anticorrelation between the two cavity modes. A quantitative measure of this anticorrelation is given by the cross-correlation function defined by

$$\delta_{\rm cross}\equiv\frac{\langle n_1n_2\rangle-\langle n_1\rangle\langle n_2\rangle}{\langle n_1\rangle\langle n_2\rangle}. \tag{53}$$

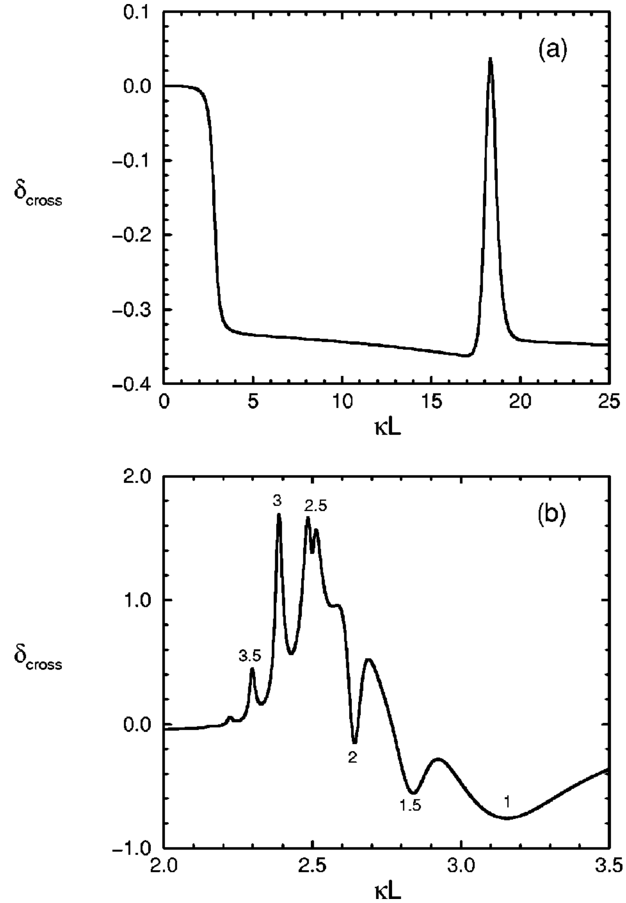

FIG. 10. The dependence of the normalized cross-correlation function on the interaction length κL for the parameters $r/C=100$, $n_b=0.1$, and (a) $k/\kappa=10$, (b) $k/\kappa=0.01$. For the case of ultracold incident atoms, the graph shows resonances at $\kappa L=m\pi/\sqrt[4]{N}$. The resonance sequence corresponding to $m=1$ has been plotted and the peaks are labeled by N values.

By using Eqs. (41) and (45), we can easily show that

$$\langle n_1n_2\rangle\equiv\sum_{n_1,n_2=0}^{\infty}n_1n_2P(n_1,n_2)=\frac{1}{6}(\langle n_\Sigma^2\rangle-\langle n_\Sigma\rangle). \tag{54}$$

Substituting Eqs. (51) and (54) into Eq. (53), we get

$$\delta_{\rm cross}=\frac{2}{3}\left(\frac{\langle n_\Sigma^2\rangle}{\langle n_\Sigma\rangle^2}-\frac{1}{\langle n_\Sigma\rangle}\right)-1. \tag{55}$$

Hence the normalized standard deviation σ_Σ and the normalized cross-correlation function $\delta_{\rm cross}$ are related by [10]

$$\sigma_\Sigma^2\equiv\frac{\langle n_\Sigma^2\rangle-\langle n_\Sigma\rangle^2}{\langle n_\Sigma\rangle}=1+\frac{3}{2}\langle n_\Sigma\rangle\left(\delta_{\rm cross}+\frac{1}{3}\right). \tag{56}$$

According to this relation, the distribution of the total number of photons in the cavity obeys sub-Poissonian statistics ($\sigma_\Sigma^2<1$) when the two cavity modes are strongly anticorrelated ($\delta_{\rm cross}<-\frac{1}{3}$). In Fig. 10, we display the normalized cross-correlation function $\delta_{\rm cross}$ as a function of κL for

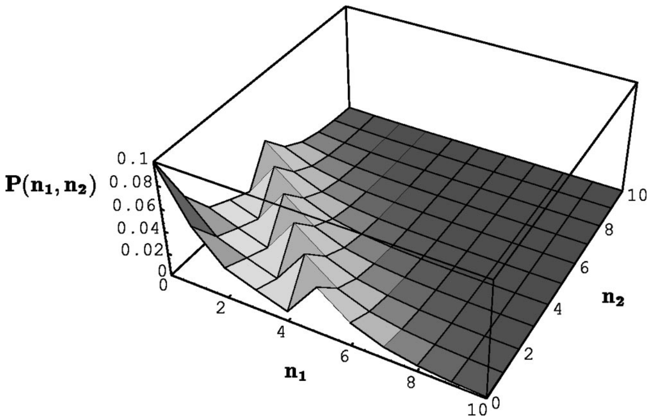

FIG. 11. The joint probability distribution $P(n_1,n_2)$ for the parameters $g_1=g_2=g$, $C_1=C_2=C$, $n_{b_1}=n_{b_2}=n_b$, $r/C=100$, $n_b=1$, $k/\kappa=0.01$, and $\kappa L=10\pi/\sqrt[4]{3}$.

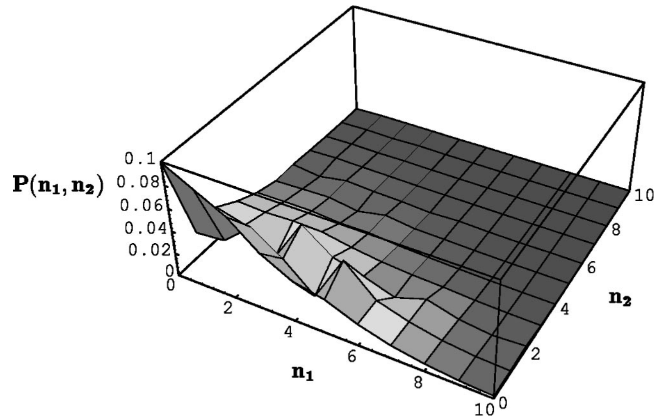

FIG. 12. The joint distribution of photons in the modes for the same parameters of Fig. 11 with $r/C=1000$, $g_2/g_1=2$.

the parameters $r/C=100$, $n_b=0.1$ both for fast atoms ($k/\kappa=10$) and for cold atoms ($k/\kappa=0.01$). It is seen from the graph that there exists a very strong anticorrelation between the cavity modes for ultracold incident atoms compared to fast atoms when $\kappa L=m\pi$ and this leads to sub-Poissonian photon statistics for the total number of photons in the cavity.

VII. JOINT DISTRIBUTION OF PHOTONS

In this section, we discuss the joint distribution of photons in the two modes of the cavity field in steady state. For the case of equal parameters $g_1=g_2=g$, $n_{b_1}=n_{b_2}=n_b$, $C_1=C_2=C$, the detailed balance steady state solution has been obtained in Sec. V. Using Eq. (41), the joint distribution of photons $P(n_1,n_2)$ is plotted in Fig. 11 for the parameters $r/C=100$, $n_b=1$, $\kappa L=10\pi/\sqrt[4]{3}$, $k/\kappa=0.01$. The graph shows that $P(n_1,n_2)$ is a symmetric function of n_1 and n_2. For the case of unequal coupling constants, i.e., $g_1\neq g_2$, the detailed balance solution does not exist. In this case, by direct integration of the rate equation (33), we have obtained the result shown in Fig. 12.

VIII. SUMMARY

The master equation for the reduced density operator of the field in the two-mode micromaser pumped by ultracold Λ-type three-level atoms has been derived and the steady state photon probability distribution under the principle of detailed balance is obtained. The interesting feature is that the degree of anticorrelation between the cavity modes increases when the micromaser is pumped by ultracold atoms instead of fast atoms. This leads to sub-Poissonian statistics for the distribution of total number of photons in the cavity. By direct integration of the rate equation for $P(n_1,n_2)$, the steady state photon probability distribution has also been obtained for the case of unequal coupling constants $g_1\neq g_2$. Further an initial asymmetric excitation of the atom-cavity system can be used to extract phase information.

[1] D. Meschede, H. Walther, and G. Müller, Phys. Rev. Lett. **54**, 551 (1985); G. Rempe, F. Schmidt-Kaler, and H. Walther, *ibid.* **64**, 2783 (1990).
[2] A recent review is given by G. Raithel, C. Wagner, H. Walther, L.M. Narducci, and M.O. Scully, in *Cavity Quantum Electrodynamics*, edited by P.R. Berman (Academic, Boston, 1994), p. 57.
[3] P. Filipowicz, J. Javanainen, and P. Meystre, Phys. Rev. A **34**, 3077 (1986).
[4] L.A. Lugiato, M.O. Scully, and H. Walther, Phys. Rev. A **36**, 740 (1987).
[5] P. Meystre, G. Rempe, and H. Walther, Opt. Lett. **13**, 1078 (1988).
[6] M.O. Scully, H. Walther, G.S. Agarwal, Tran Quang, and W. Schleich, Phys. Rev. A **44**, 5992 (1991).
[7] M. Weidinger, B.T.H. Varcoe, R. Heerlein, and H. Walther, Phys. Rev. Lett. **82**, 3795 (1999).
[8] M. Brune, J.M. Raimond, P. Goy, L. Davidovich, and S. Haroche, Phys. Rev. Lett. **59**, 1899 (1987).
[9] K. An, J.J. Childs, R.R. Dasari, and M.S. Feld, Phys. Rev. Lett. **73**, 3375 (1994).
[10] Fam Le Kien, G.M. Meyer, M.O. Scully, H. Walther, and Shi-Yao Zhu, Phys. Rev. A **49**, 1367 (1994).
[11] Laser-cooling techniques are reviewed in *Laser Manipulation of Atoms and Ions*, edited by E. Arimondo, W.D. Phillips, and F. Strumia (North-Holland, Amsterdam, 1992).
[12] B.G. Englert, J. Schwinger, A.O. Barut, and M.O. Scully, Europhys. Lett. **14**, 25 (1991).
[13] S. Haroche, M. Brune, and J.M. Raimond, Europhys. Lett. **14**, 19 (1991).
[14] M.O. Scully, G.M. Meyer, and H. Walther, Phys. Rev. Lett. **76**, 4144 (1996).
[15] G.M. Meyer, M.O. Scully, and H. Walther, Phys. Rev. A **56**, 4142 (1997).

[16] M. Löffler, G.M. Meyer, M. Schröder, M.O. Scully, and H. Walther, Phys. Rev. A **56**, 4153 (1997).
[17] M. Schröder, K. Vogel, W.P. Schleich, M.O. Scully, and H. Walther, Phys. Rev. A **56**, 4164 (1997).
[18] Ching Tsung Lee, J. Opt. Soc. Am. B **14**, 1576 (1997).
[19] Zhi-Ming Zhang, Zhi-Yuan Lu, and Lin-Sheng He, Phys. Rev. A **59**, 808 (1999).
[20] Zhi-Ming Zhang and Lin-Sheng He, Opt. Commun. **157**, 77 (1998).